

How the Kondo ground state avoids the orthogonality catastrophe

Gerd Bergmann
Department of Physics
University of Southern California
Los Angeles, California 90089-0484
e-mail: bergmann@usc.edu

November 4, 2018

Abstract

In the presence of a magnetic impurity the spin-up and down band states are modified differently by the impurity. If the multi-electron scalar product (MESP) between the occupied spin-up and down states approaches zero then this defines an orthogonality catastrophe. In the present paper the MESP is investigated for the FAIR (**F**riedel **A**rtificial **I**serted **R**esonance) solution for a Friedel-Anderson impurity. A basis of Wilson states is used. The MESP is numerically determined for the (enforced) magnetic, the singlet, and the triplet states as a function of the number N of Wilson states. The magnetic and the triplet state show an exponentially decreasing MESP as a function of N . Surprisingly it is not the number of states which causes this decrease. It is instead the energy separation of the highest occupied state from the Fermi energy which determines the reduction of the MESP. In the singlet state the ground-state requires a finite MESP to optimize its energy. As a consequence there is no orthogonality catastrophe. The MESP approaches a saturation value as function of N .

PACS: 75.20.Hr, 71.23.An, 71.27.+a

1 Introduction

The orthogonality (or infrared) catastrophe was introduced and discussed already 40 years ago [1], [2], [3], [4]. An example is a magnetic impurity in a metal host which interacts with the conduction electron in the form $H' = 2J(\mathbf{r})\mathbf{s} \cdot \mathbf{S}$. The effect of the z-component $2J(\mathbf{r})s_z S_z$ is the following. Let the spin direction of the impurity point upwards. Then the wave function of the conduction electrons is pulled towards or pushed away from the impurity, depending on the electron spin. As a consequence the scalar product of corresponding s-electron states with opposite spin is slightly less than 1.

If we denote the resulting (modified) bases for spin up and down as $\{c_{\nu+}^\dagger\}$ and $\{c_{\nu-}^\dagger\}$ with N states in each basis ($1 \leq \nu < N$) and if the lowest $N/2$ states are occupied then the value of the multi-electron scalar product (**MESP**) between all occupied s-states with spin up and those with spin down is defined by the determinant

$$M^{N/2} = \begin{vmatrix} \langle c_{1,+}^\dagger | c_{1,-}^\dagger \rangle & \langle c_{1,+}^\dagger | c_{N/2,-}^\dagger \rangle \\ \langle c_{N/2,+}^\dagger | c_{1,-}^\dagger \rangle & \langle c_{N/2,+}^\dagger | c_{N/2,-}^\dagger \rangle \end{vmatrix}$$

The common argument is that the multi-electron scalar product between all occupied s-states with spin up and those with spin down approaches zero when the number of occupied s-electron states approaches zero. If one complements this system of impurity with spin up plus polarized conduction electrons with the time reversed system where all spin directions are reversed then a transition between the two by spin-flip processes of the form $J(\mathbf{r})[s^+ S^- + s^- S^+]$ has vanishing amplitude. Therefore the non-diagonal part of the $\mathbf{s} \cdot \mathbf{S}$ interaction tries to prevent the orthogonality catastrophe. This can be well traced in the Fair treatment of the Kondo impurity.

In the following the Friedel-Anderson (FA) impurity will be discussed where this process is less obvious. The Hamiltonian for the FA-impurity is given by

$$H_{FA} = \sum_{\sigma} \left\{ \sum_{\nu=1}^N \varepsilon_{\nu} c_{\nu,\sigma}^\dagger c_{\nu,\sigma} + E_d d_{\sigma}^\dagger d_{\sigma} + \sum_{\nu=1}^N V_{sd}(\nu) [d_{\sigma}^\dagger c_{\nu,\sigma} + c_{\nu,\sigma}^\dagger d_{\sigma}] \right\} + U n_{d\uparrow} n_{d\downarrow} \quad (1)$$

During the past few years the author has introduced a new numerical approach to the Kondo and the FA-impurity problem, the FAIR-method (Friedel Artificially Inserted Resonance) [5], [6][7]. It is based on the fact the n -electron ground state of the Friedel Hamiltonian (consisting of an electron band and a d-resonance) can be exactly expressed as the sum of two Slater states [8]

$$\Psi_{Fr} = A a_0^\dagger \prod_{i=1}^{n-1} a_i^\dagger \Phi_0 + B d^\dagger \prod_{i=1}^{n-1} a_i^\dagger \Phi_0 \quad (2)$$

where a_0^\dagger is an artificial Friedel resonance state which determines uniquely the full orthonormal basis $\{a_i^\dagger\}$. An extension of this ground state to the Friedel-Anderson and Kondo

impurity problem yields good numerical results. Recently this method was applied to calculate the Kondo polarization cloud for those impurities [9].

Three different solutions of the FA-Hamiltonian will be discussed: the magnetic state, the singlet state and the triplet state. For sufficiently large U this Hamiltonian yields a magnetic state at temperature only above the Kondo temperature T_K . However, a magnetic state can be enforced by the structure of the variational state. This state will be called the *enforced magnetic state*. This avoids the finite temperature treatment. This magnetic solution Ψ_{MS} has the form

$$\Psi_{MS} = \left[A a_{0-\downarrow}^\dagger a_{0+\uparrow}^\dagger + B d_{\downarrow}^\dagger a_{0+\uparrow}^\dagger + C a_{0-\downarrow}^\dagger d_{\uparrow}^\dagger + D d_{\downarrow}^\dagger d_{\uparrow}^\dagger \right] \prod_{i=1}^{n-1} a_{i-\downarrow}^\dagger \prod_{i=1}^{n-1} a_{i+\uparrow}^\dagger \Phi_0 \quad (3)$$

The coefficients A, B, C, D and the compositions of the FAIR states a_{0+}^\dagger and a_{0-}^\dagger are optimized to minimize the energy expectation value of the FA Hamiltonian. Due to the condition $\langle a_{i\tau}^\dagger \Phi_0 | H_0 | a_{j\tau}^\dagger \Phi_0 \rangle = 0$ for $i, j > 0$ and $\tau = +, -$ the FAIR states determine the other states $a_{i\tau}^\dagger$ of the basis $\{a_{i\tau}^\dagger\}$ uniquely.

The singlet state is a symmetric superposition of a magnetic state and its time- (or spin-) reversed state, while the triplet state is the asymmetric superposition. (The FAIR states a_{0+}^\dagger and a_{0-}^\dagger and the coefficients A, B, C, D are independently optimized for the magnetic, singlet, and triplet states).

For the Fair solution the MESP between the occupied spin up and spin down sub-bands is essentially given by

$$M_{+-}^{(N/2)} = \left\langle \prod_{i=0}^{N/2-1} a_{i+}^\dagger \Phi_0 \middle| H_0 \middle| \prod_{j=0}^{N/2-1} a_{j-}^\dagger \Phi_0 \right\rangle \quad (4)$$

2 Numerical Calculation of the Multi-Electron Scalar Product

2.1 The enforced magnetic state

For most of the numerical calculations Wilson states are used (see appendix A). In the calculation the following parameters are used: $|V_{sd}|^2 = 0.1$, $U = 1$, $E_d = -0.5$. The magnetic solution is optimized for different numbers of Wilson states with $N = 20, 30, 40, 50, 60$. Table I shows $M_{MS}^{(N/2)}$ of the magnetic solution for the different sizes N of the bases. The third column gives the scalar product of the two FAIR states, $\langle a_{0+} \Phi_0 | a_{0-} \Phi_0 \rangle_{MS}$, the fourth column the ground-state energy, and the fifth column gives the magnetic moment. (Φ_0 is the vacuum state). As one can see the scalar product $\langle a_{0+} \Phi_0 | a_{0-} \Phi_0 \rangle_{MS}$, the ground-state energy (in the

enforced magnetic state), and the moment have reached their final values already for $N = 30$. However, the multi-scalar product decreases with increasing N .

N	$M_{MS}^{(N/2)}$	$\langle a_{0+} a_{0-}\rangle_{MS}$	$E_{0,MS}$	μ	$\langle a_{N/2} a_{N/2}\rangle_{MS}$
10	0.878	0.823	-0.607799	0.514	.92(.25)
20	0.396	0.501	-0.627446	0.687	.64(.65)
30	0.190	0.4852	-0.62810	0.690	.55(.69)
40	0.0917	0.4845	-0.62812	0.690	.52(.76)
50	0.0443	0.4845	-0.62812	0.690	.50(.77)
60	0.0216	0.484	-0.62812	0.690	.49(.79)
2*20	0.394	0.526	-0.629323	0.66	.64(.61)
2*30	0.198	0.514	-0.629779	0.67	.57(.70)

Table I: The multi-electron scalar product (MESP) and other parameters for the Friedel-Anderson impurity in the enforced magnetic state. The different columns give the number of Wilson states, the MESP, the (single electron) scalar product $\langle a_{0+}\Phi_0|a_{0-}\Phi_0\rangle_{MS}$ between the two FAIR states, the ground-state energy, and the magnetic moment. The 6th column is explained in the text. The parameters used in the calculation are $|V_{sd}|^2 = 0.1$, $U = 1$, $E_d = -0.5$.

In Fig.1 the logarithm of the multi-electron scalar product $\ln(M_{MS}^{(N/2)})$ is plotted versus the number of Wilson states N . It follows a straight line which corresponds to the relation

$$M_{MS}^{(N/2)} = 1.7e^{-0.073*N} = 1.7 * 0.93^{-N}$$

Obviously, the multi-scalar product decreases exponentially with increasing N .

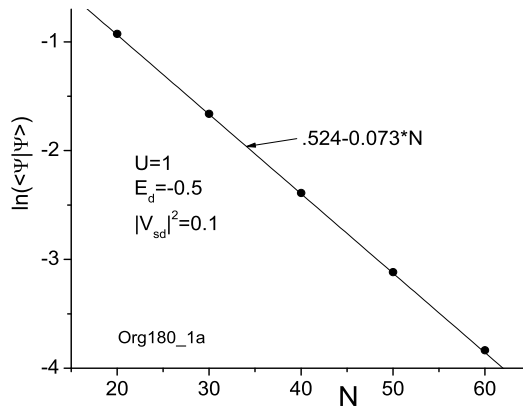


Fig.1: The logarithm of the multi-electron scalar product MESP $\langle \prod_{i=0}^{n-1} a_{i+}^\dagger \Phi_0 | \prod_{i=0}^{n-1} a_{i-}^\dagger \Phi_0 \rangle$ is plotted versus the number of Wilson states N with $n = N/2$ for the magnetic state.

In the next step I check whether it is just the number of states N which reduces $M_{MS}^{(N/2)}$. For this purpose the N energy cells for $N = 20$ and 30 are sub-divided into two. This is achieved by using $\Lambda = \sqrt{2}$. This doubles the number of Wilson states but adds only one state (for positive and negative energy) closer to the Fermi level. The results of this calculation are collected at $N = 2 * 20$ and $2 * 30$. It turns out that the doubling has essentially only a minor effect on $M_{MS}^{(N/2)}$. This is on a first sight rather surprising since it was believed that the increase of the number of states causes the orthogonality catastrophe of the MESP.

To further confirm this observation I take the energy frame with $N = 20$ and subdivide the energy range $(-1 : -1/4)$ into cells with a width of $1/8$, replacing two Wilson states by six new states. (The same is done for the positive range). This changes $M_{MS}^{N/2}$ from 0.396 to 0.405 . Splitting the same energy range into 14 cells with a width of $1/32$ yields the MESP $M_{MS}^{N/2} = 0.411$. This shows that increasing N by subdividing an energy range does not contribute to an orthogonality catastrophe (as long as the energy range does not border the Fermi level at the energy 0).

On the other hand, the smallest (absolute) energies have a great impact on the MESP. To investigate this question further I take the energies for $N = 20$ and shift the two states which are closest to the Fermi level towards the Fermi level. The four energy cells which are closest to the Fermi level are $\mathfrak{C}_9 = (-2^{-8} : -2^{-9})$, $\mathfrak{C}_{10} = (-2^{-9} : 0)$, $\mathfrak{C}_{11} = (0 : 2^{-9})$, $\mathfrak{C}_{12} = (2^{-9} : 2^{-8})$. I replace $\pm 2^{-9}$ by $\pm 2^{-19}$. Then the (average) energies of the corresponding states are $\varepsilon_9 = -\frac{2049}{1048576} \approx -1.9541 \times 10^{-3}$, $\varepsilon_{10} = -2^{-20}$, $\varepsilon_{11} = 2^{-20}$ and $\varepsilon_{12} = 1.9541 \times 10^{-3}$. Of course this reduces the s-d interaction strength $V_{sd}(\nu)$ for $\nu = 10, 11$ from $[2^{-9}/2]^{1/2} = 2^{-5}$ to $[2^{-19}/2]^{1/2} = 2^{-10}$. (The ratio $|V_{sd}(\nu)|^2 / \varepsilon_\nu$ remains constant).

After optimizing the $\{a_{i+}\}$ and $\{a_{i-}\}$ bases and the coefficients A, B, C, D the resulting MESP is reduced to $M_{MS}^{10} = 0.0208$. The number of states is still $N = 20$. The shifting of the smallest energies from $\pm 2^{-10}$ to $\pm 2^{-20}$ changes the value of the MESP from 0.396 to 0.0208 . This shows that the value of the MESP is determined by the occupied state closest to the Fermi level. The total number of states is only important when it determines the energy of this state.

2.2 The singlet state

In the next step I calculate the MESP for the singlet ground state. The same parameters $|V_{sd}|^2 = 0.1$, $U = 1$, $E_d = -0.5$ are used as in table I and Fig.1. The FAIR solution for the singlet state is obtained by reversing all spins in Ψ_{MS} and combining the two states.

$$\Psi_{SS} = \Psi_{MS}(\uparrow\downarrow) + \Psi_{MS}(\downarrow\uparrow)$$

$$\begin{aligned}
&= \left[Aa_{0-\downarrow}^\dagger a_{0+\uparrow}^\dagger + Bd_{\downarrow}^\dagger a_{0+\uparrow}^\dagger + Ca_{0-\downarrow}^\dagger d_{\uparrow}^\dagger + Dd_{\downarrow}^\dagger d_{\uparrow}^\dagger \right] \prod_{i=1}^{n-1} a_{i-\downarrow}^\dagger \prod_{i=1}^{n-1} a_{i+\uparrow}^\dagger \Phi_0 \\
&+ \left[A'a_{0-\uparrow}^\dagger a_{0+\downarrow}^\dagger + B'd_{\uparrow}^\dagger a_{0+\downarrow}^\dagger + C'a_{0-\uparrow}^\dagger d_{\downarrow}^\dagger + D'd_{\uparrow}^\dagger d_{\downarrow}^\dagger \right] \prod_{i=1}^{n-1} a_{i-\uparrow}^\dagger \prod_{i=1}^{n-1} a_{i+\downarrow}^\dagger \Phi_0
\end{aligned} \tag{5}$$

The coefficients $A, B, C, D, A', B', C', D'$ and the compositions of the FAIR states a_{0+}^\dagger and a_{0-}^\dagger are again optimized to minimize the energy expectation value of the FA Hamiltonian. In table II are the corresponding data collected. Again the first four columns give the same data as in table I, i.e. the number of Wilson states, the MESP, the (single electron) scalar product between the two FAIR states a_{0+}^\dagger and a_{0-}^\dagger and the ground-state energy. The 5th column gives the Kondo energy (difference between the relaxed triplet energy and the singlet ground-state energy).

Dependence on the number of states N

N	$M_{SS}^{(N/2)}$	$\langle a_{0+} a_{0-} \rangle_{SS}$	$E_{0,SS}$	ΔE	$>.999$
10	0.749	0.645	-0.62272	14.8×10^{-3}	
20	0.742	0.6448	-0.637535	10.1×10^{-3}	9-10
30	0.742	0.6448	-0.637965	9.87×10^{-3}	9-21
40	0.742	0.6448	-0.63798	9.86×10^{-3}	9-31
50	0.742	0.6448	-0.63798	9.86×10^{-3}	9-41
60	0.742	0.6448	-0.637973	9.85×10^{-3}	9-51
2*20	0.751	0.657	-0.639684	10.4×10^{-3}	17-23
2*30	0.751	0.657	-0.639993	10.2×10^{-3}	18-43

Table II: The multi-electron scalar product (MESP) and other parameters for the Friedel-Anderson impurity in the singlet state. The different columns give the number of Wilson states N , the MESP, the (single electron) scalar product $\langle a_{0+} \Phi_0 | a_{0-} \Phi_0 \rangle_{MS}$ between the two FAIR states, the ground-state energy, and the Kondo energy. The 6th column is explained in the text. The parameters used in the calculation are $|V_{sd}|^2 = 0.1$, $U = 1$, $E_d = -0.5$.

For the last column I calculated the scalar product $\langle a_{+,i}^\dagger \Phi_0 | a_{-,j}^\dagger \Phi_0 \rangle$ for all pairs of (i, j) which form a $N \times N$ -matrix. It turns out that the diagonal elements $\langle a_{+,i}^\dagger \Phi_0 | a_{-,i}^\dagger \Phi_0 \rangle$ close to the Fermi energy approach the value one. For example if the sixth column shows for $N = 30$ the value "9 - 21" then the values of the (single particle) scalar products $\langle a_{+,i}^\dagger \Phi_0 | a_{-,i}^\dagger \Phi_0 \rangle$ lie between 0.999 and 1.000 for $9 \leq i \leq 21$. Obviously the states $a_{+,i}^\dagger$ and $a_{-,i}^\dagger$ are almost identical in this interval. This is very different for the enforced magnetic state. There, in table I the 6th column shows the value of the diagonal scalar product for $i = N/2$ and the larger one of its two neighbors $\langle a_{+,N/2}^\dagger \Phi_0 | a_{-,N/2\pm 1}^\dagger \Phi_0 \rangle$.

Dependence on the interaction $|V_{sd}|^2$

The MESP in the singlet state depends on the strength of the s-d interaction. Keeping the number of Wilson states constant $N = 40$ the MESP is numerically determined and collected in table III.

$ V_{sd} ^2$	$M_{SS}^{(N/2)}$	$\langle a_{0+}^\dagger a_{0-}^\dagger \rangle_{SS}$	$E_{0,SS}$	ΔE	>.999
0.10	0.742	0.645	-0.637977	9.86×10^{-3}	-
0.09	0.708	0.604	-0.621392	8.13×10^{-3}	10-30
0.08	0.665	0.553	-0.605078	6.14×10^{-3}	10-30
0.07	0.607	0.489	-0.589200	4.09×10^{-3}	11-29
0.06	0.527	0.406	-0.573975	2.22×10^{-3}	11-29
0.05	0.407	0.299	-0.559655	8.21×10^{-4}	12-28

Table III: The multi-electron scalar product (MESP) and other parameters for the Friedel-Anderson impurity in the singlet state. The columns give the s-d interaction $|V_{sd}|^2$, the MESP, the scalar product $\langle a_{0+}^\dagger \Phi_0 | a_{0-}^\dagger \phi_0 \rangle$, the ground-state energy, and Kondo energy ΔE . The 6th column is explained in the text. The parameters used in the calculation are $U = 1$, $E_d = -0.5$ and the number of Wilson states is $N = 40$.

In Fig.2 the logarithm of the Kondo energy is plotted versus the logarithm of the MESP. A linear dependence is obtained. The MESP shows a weak dependence on the Kondo energy with a power of about 1/4.

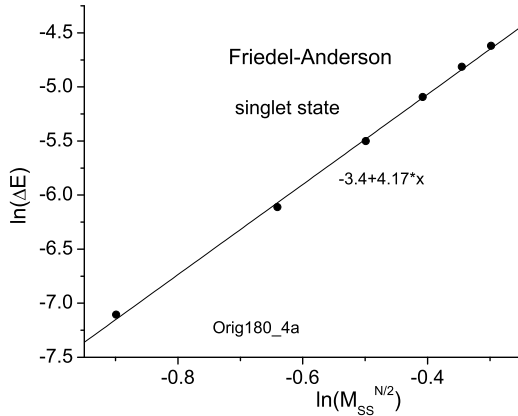


Fig.2: The log-log plot of the Kondo energy versus the MESP for the singlet state for different s-d interactions.

2.3 The triplet state

If one arranges the spins in each component in equ. (5) for the singlet state so that all spin-down creation operators are moved to the left and all spin-up ones to the right, then the coefficients are pair-wise equal, i.e. $A' = A$, $B' = B$, etc. This yields the symmetric or singlet state. On the other hand, if one sets the coefficients pair-wise opposite equal, i.e. $A' = -A$, $B' = -B$, etc then one obtains the asymmetric or triplet state. Of course, one has to restart the optimization of $a_{0,+}^\dagger$, $a_{0,-}^\dagger$ and A, B, C, D . For the asymmetric state a finite MESP increases the total energy. So if one searches for the relaxed triplet state with minimal energy one may expect a strong reduction of the MESP. This is indeed found. In table III the data for the triplet state are collected for the same parameters as before.

N	$M_{TS}^{(N/2)}$	$\langle a_{0,+}^\dagger a_{0,-}^\dagger \rangle_{TS}$	$E_{0,SS}$	$\langle a_{N/2} a_{N/2} \rangle_{TS}$
10	0.926	0.891	-0.582822	.97(.12)
20	0.0998	0.448	-0.626428	.16(.85)
30	0.0162	0.481	-0.628054	.049(.88)
40	2.59×10^{-3}	0.484	-0.628117	.020(.89)
50	3.02×10^{-4}	0.484	-0.628119	.082(.96)
60	4.17×10^{-5}	0.484	-0.628119	.21(.95)

Table III: The multi-electron scalar product (MESP) and other parameters for the Friedel-Anderson impurity in the triplet state. The columns give the number of Wilson states N , the MESP, $\langle a_{0,+}^\dagger | \Phi_0 | a_{0,-}^\dagger | \Phi_0 \rangle$, and the ground-state energy. The last column is explained in the text. The parameters used in the calculation are $|V_{sd}|^2 = 0.1$, $U = 1$, $E_d = -0.5$.

In the limit of large N the MESP approaches zero. That means that the two components in equ. (5) (top and the bottom line) are completely decoupled. The triplet state consists of two orientations of the magnetic state with zero interaction between them. Therefore the energies in the magnetic and the triplet state become equal for large N . A comparison between table I and table III does indeed show this agreement.

The dependence of the logarithm of the MESP on the number N of Wilson states is

plotted in Fig.3.

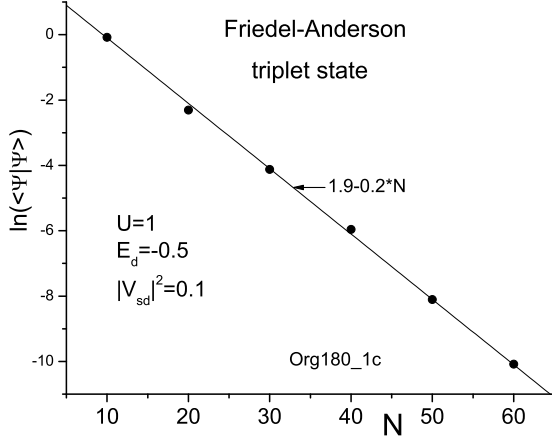


Fig.3: The logarithm of the MESP $\langle \prod_{i=0}^{n-1} a_{i+}^\dagger \Phi_0 | \prod_{i=0}^{n-1} a_{i-}^\dagger \Phi_0 \rangle$ is plotted versus the number of Wilson states N with $n = N/2$ for the triplet state

3 Discussion and Conclusion

The states $a_{+,i}^\dagger$ are constructed from the basis c_ν^\dagger by extracting a FAIR state $a_{+,0}^\dagger$. Therefore the states $a_{+,i}^\dagger$ and c_ν^\dagger are pair-wise quite similar except that there is one state missing in the basis $\{a_{+,i}\}$.

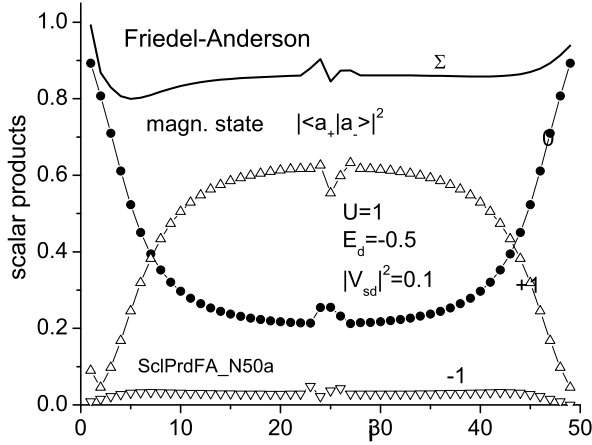


Fig.4: The square of the diagonal matrix-elements $\left| \langle a_{+,i}^\dagger \Phi_0 | a_{-,i}^\dagger \Phi_0 \rangle \right|^2$ as well as the next-to-diagonal matrix-elements $\left| \langle a_{+,i}^\dagger \Phi_0 | a_{-,i\pm 1}^\dagger \Phi_0 \rangle \right|^2$ are plotted as a function of i for the enforced magnetic state.

As a consequence the two bases $\{a_{+,i}^\dagger\}$ and $\{a_{-,i}^\dagger\}$ are quite similar. In Fig.4 the single-particle scalar products $\left| \langle a_{+,i}^\dagger \Phi_0 | a_{-,j}^\dagger \Phi_0 \rangle \right|^2$ for the enforced magnetic state are plotted as

a function of i (full circles). In addition $\left| \left\langle a_{+,i}^\dagger \Phi_0 | a_{-,i\pm 1}^\dagger \Phi_0 \right\rangle \right|^2$ are plotted as empty up and down triangles. The full curve (without symbols) gives the sum of the three contributions. One recognizes that an arbitrary state $a_{+,i}^\dagger$ (for $i > 0$) can be constructed to 80% out of the states $a_{-,i}^\dagger$, $a_{-,i+1}^\dagger$ and $a_{-,i-1}^\dagger$. On the other hand $a_{+,i}^\dagger$ and $a_{-,i}^\dagger$ overlap to only 30% for small energies (in the center of the horizontal axis).

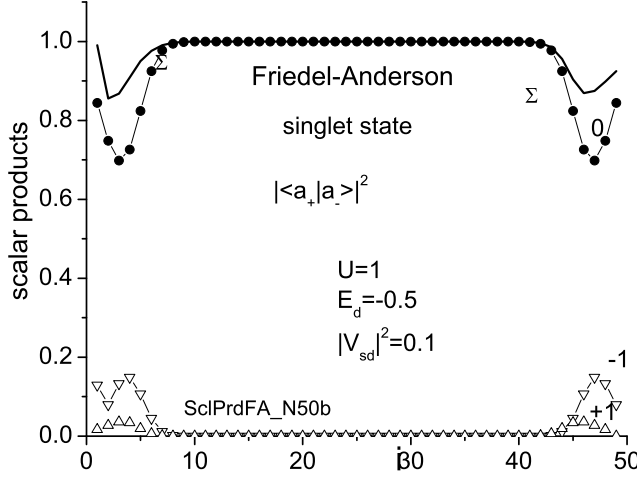


Fig.5: The square of the diagonal matrix-elements $\left| \left\langle a_{+,i}^\dagger \Phi_0 | a_{-,i}^\dagger \Phi_0 \right\rangle \right|^2$ as well as the next-to-diagonal matrix-elements $\left| \left\langle a_{+,i}^\dagger \Phi_0 | a_{-,i\pm 1}^\dagger \Phi_0 \right\rangle \right|^2$ are plotted as a function of i for the singlet state.

This is very different for the singlet state. In Fig.5 the single-electron scalar products $\left| \left\langle a_{+,i}^\dagger \Phi_0 | a_{-,i}^\dagger \Phi_0 \right\rangle \right|^2$ as well as $\left| \left\langle a_{+,i}^\dagger \Phi_0 | a_{-,i\pm 1}^\dagger \Phi_0 \right\rangle \right|^2$ are plotted as a function of i for the singlet state. One recognizes that over a large energy range the states $a_{+,i}^\dagger$ and $a_{-,i}^\dagger$ are 99% or more identical. Only for (absolute) larger energies on the left and right side is the overlap reduced to about 70%.

The reason for this different behavior is rather transparent. The energy expectation value of the enforced magnetic state does not depend on the MESP. The s-d transitions happen only within the same spin orientation and therefore between the same bases. As an example, one has the transition

$$a_{0-\downarrow}^\dagger d_{\uparrow}^\dagger \prod_{i=1}^{n-1} a_{i-\downarrow}^\dagger \prod_{i=1}^{n-1} a_{i+\uparrow}^\dagger \Phi_0 \iff d_{\downarrow}^\dagger d_{\uparrow}^\dagger \prod_{i=1}^{n-1} a_{i-\downarrow}^\dagger \prod_{i=1}^{n-1} a_{i+\uparrow}^\dagger \Phi_0$$

Here the matrix element is just

$$\begin{aligned} & \left\langle a_{0-\downarrow}^\dagger d_{\uparrow}^\dagger \prod_{i=1}^{n-1} a_{i-\downarrow}^\dagger \prod_{i=1}^{n-1} a_{i+\uparrow}^\dagger \Phi_0 \left| V_{sd}^-(0) a_{0,\downarrow}^\dagger d_{\downarrow} \right| d_{\downarrow}^\dagger d_{\uparrow}^\dagger \prod_{i=1}^{n-1} a_{i-\downarrow}^\dagger \prod_{i=1}^{n-1} a_{i+\uparrow}^\dagger \Phi_0 \right\rangle \\ & = \left\langle a_{0-\downarrow}^\dagger \Phi_0 \left| V_{sd}^-(0) a_{0,\downarrow}^\dagger d_{\downarrow} \right| d_{\downarrow}^\dagger \Phi_0 \right\rangle = V_{sd}^-(0) \end{aligned}$$

With $a_{0-}^\dagger = \sum_{\nu=1}^N \alpha_{0-}^\nu c_\nu^\dagger$ the value of $V_{sd}^-(0)$ is given by

$$V_{sd}^-(0) = \sum_{\nu=1}^N \alpha_{0-}^\nu V_{sd}(\nu)$$

There are no processes that involve the MESP.

On the other hand in the singlet state one has transitions from

$$a_{0-\downarrow}^\dagger a_{0+\uparrow}^\dagger \prod_{i=1}^{n-1} a_{i-\downarrow}^\dagger \prod_{i=1}^{n-1} a_{i+\uparrow}^\dagger \Phi_0 \Leftrightarrow a_{0+\downarrow}^\dagger a_{0-\uparrow}^\dagger \prod_{i=1}^{n-1} a_{i-\uparrow}^\dagger \prod_{i=1}^{n-1} a_{i+\downarrow}^\dagger \Phi_0$$

Such a transition is proportional to the square of the MESP. To be able to harvest energy from these processes the states a_{i+}^\dagger and a_{i-}^\dagger are, for small energies, aligned parallel to each other.

In Fig.6 the corresponding single-particle scalar products $\left| \langle a_{+,i}^\dagger \Phi_0 | a_{-,j}^\dagger \Phi_0 \rangle \right|^2$ for the triplet state are plotted as a function of i . With exception of the few (2 - 4) points in the center the results is very close to the result of the enforced magnetic state. The two (magnetic) components of the triplet state are essentially decoupled because the coupling is proportional to $[M^{(N/2)}]^2$ which is of the order of 10^{-7} . Therefore the triplet state is essentially equal to the sum of the enforced magnet state plus its time- (spin-) reversed partner (for sufficiently large N).

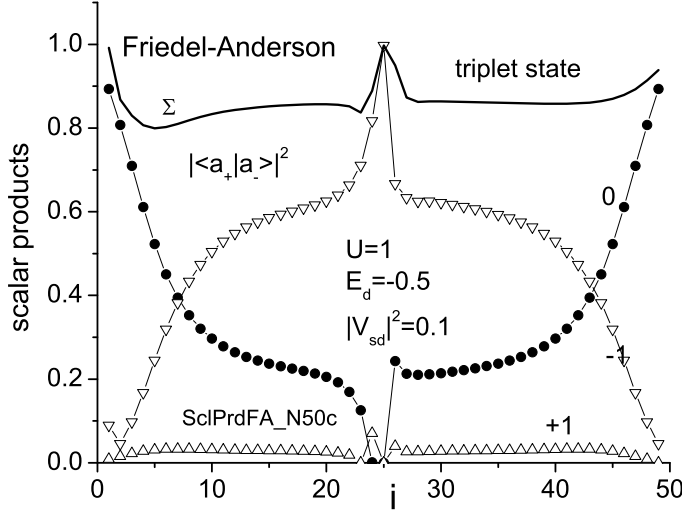


Fig.6: The square of the diagonal matrix-elements $\left| \langle a_{+,i}^\dagger \Phi_0 | a_{-,i}^\dagger \Phi_0 \rangle \right|^2$ as well as the next-to diagonal matrix-elements $\left| \langle a_{+,i}^\dagger \Phi_0 | a_{-,i\pm 1}^\dagger \Phi_0 \rangle \right|^2$ are plotted as a function of i for the triplet state.

The results of this paper are two-fold. One has to distinguish whether (the expectation value of) the energy in the ground state depends on the MESP. If E_0 is independent of the MESP and one uses the Wilson states as the original basis then the MESP $M^{N/2}$ decreases exponentially with increasing N . This is due to the fact that the energy of the states closest to the Fermi level decreases exponentially as well. Just by moving these states closer

decreases $M^{N/2}$. On the other hand if the total number of states in a given energy interval is increased without reducing the energy of the states closest to the Fermi energy then the MESP $M^{N/2}$ is barely affected.

If the energy in the ground state depends on the MESP (as for the singlet state) then this results in a freeze of the MESP. This achieved by forcing the new basis states $a_{i,+}^\dagger$ and $a_{i,-}^\dagger$ to be parallel within a certain energy range of the Fermi level.

4 Appendix

A Wilson states

Wilson [10] in his Kondo paper considered an s-band ranging from -1 to 1 with a constant density of states. In the next step Wilson replaced the energy continuum of s-states by a discrete set of cells. First the negative energy band is subdivided on a logarithmic scale. The discrete energy values are $-1, -1/2, -1/2^2, -2^{-\nu}, \dots, -2^{-(N/2-1)}, 0$. These discrete $\xi_\nu = -2^{-\nu}$ points are used to define a sequence of energy cells: the cell \mathfrak{C}_ν (for $\nu < N/2$) includes all states within $(\xi_{\nu-1} : \xi_\nu) = (-1/2^{\nu-1} : -1/2^\nu)$. A new (Wilson) state c_ν^\dagger is a superposition of all states within an energy cell $(\xi_{\nu-1} : \xi_\nu)$ and has an (averaged) energy $(\xi_{\nu-1} + \xi_\nu)/2 = \left(-\frac{3}{2}\right) \frac{1}{2^\nu}$. This yields a spectrum ε_ν : $-\frac{3}{4}, -\frac{3}{8}, -\frac{3}{16}, \dots, -\frac{3}{2^{N/2}}, -\frac{1}{2^{N/2}}$. This spectrum is extended symmetrically to positive energies (for $\nu > N/2$). The essential advantage of the Wilson basis is that it has an arbitrarily fine energy spacing at the Fermi energy. For a given N the two smallest energy cells extend from $\pm 2^{-(N/2-1)}$ to 0 , and the (absolute) smallest energy levels are $\pm 2^{-N/2}$.

References

- [1] P. W. Anderson, Phys. Rev. Lett. 18, 1049 (1967) , The orthogonality catastrophe
- [2] D. R. Hamann, Phys. Rev. Lett. 26, 1030 (1971) , Orthogonality Catastrophe in Metals
- [3] K. Yamada and K. Yosida, Prog. Theor. Phys. 59, 1061 (1979) , Orthogonality Catastrophe Due to Local Electron Interaction
- [4] K. Yamada and K. Yosida, Prog. Theor. Phys. 62, 363 (1979) , Orthogonality Catastrophe for a System of Interacting Electrons. II
- [5] G. Bergmann, Phys. Rev. B 74, 144420 (2006) , Compact Approximate Solution to the Friedel-Anderson Impurity Problem
- [6] G. Bergmann, Phys. Rev. B 73, 092418 (2006) , A Critical Analysis of the Mean-Field Approximation for the Calculation of the Magnetic Moment in the Friedel-Anderson Impurity Model
- [7] G. Bergmann and L. Zhang, Phys. Rev. B 76, 064401 (2007) , A Compact Approximate Solution to the Kondo Problem
- [8] G. Bergmann, Z. Physik B102, 381 (1997), A new many-body solution of the Friedel resonance problem
- [9] G. Bergmann, Phys. Rev. B 77, 104401 (2008) , Quantitative calculation of the spatial extension of the Kondo cloud
- [10] K. G. Wilson, Rev. Mod. Phys. 47, 773 (1975), The renormalization group: Critical phenomena and the Kondo problem